

## **Introduction to the strain-smoothed element method for analysis of solid and shell problems**

Chaemin Lee<sup>1)</sup>, Cheolgyu Hyun<sup>2)</sup>, \*Phill-Seung Lee<sup>3)</sup>

<sup>1),2),3)</sup> Department of Mechanical Engineering, KAIST, Daejeon 34141, Korea  
<sup>3)</sup> [phillseung@kaist.edu](mailto:phillseung@kaist.edu)

### **ABSTRACT**

We introduce the strain-smoothed element (SSE) method recently developed for analysis of solid and shell problems. The strain-smoothed 3-node triangular and 4-node tetrahedral solid elements and 3-node triangular shell element were developed. Unlike smoothed finite element methods (S-FEMs), the SSE method requires no special smoothing domain and linear strain fields are formed within elements. The strain-smoothed elements pass the basic tests (isotropy, patch and zero energy mode tests) and show significantly improved convergence behavior in various numerical examples. The method could be easily extended for solving non-linear problems.

### **1. INTRODUCTION**

The strain smoothing methods are effective in improving convergence behaviors of finite elements without using additional degrees of freedom (DOFs). In conventional strain smoothing methods such as the edge-based and node-based smoothed finite element methods (S-FEMs), special smoothing domains (distinct from finite elements) are required, and piecewise constant strain fields are formed in the newly constructed smoothing domains (Liu 2009, Sohn 2013, Shin 2013, Lee 2016, 2017).

Recently, a new strain smoothing method, named the strain-smoothed element (SSE) method, has been developed for 3-node triangular and 4-node tetrahedral solid elements. Unlike the conventional smoothing methods, the SSE method has the same domain discretization as the standard finite element method (FEM). Therefore, it is easy to use the SSE method in combination with the standard FEM. The smoothed elements adopting the SSE method show significantly improved convergence behaviors compared to those adopting the edge-based S-FEM in various numerical examples (Lee 2018). Also, the method has been adopted for improving the membrane performance of the MITC3+ shell element, which already showed excellent behaviors in bending-dominated problems (Lee 2019).

In the following sections, the formulation of the SSE method is reviewed for the solid and shell elements. We also demonstrate the accuracy improvement achieved through some numerical examples.

## 2. STRAIN-SMOOTHED ELEMENT METHOD FOR SOLID ELEMENTS

The geometry of the standard 3-node triangular element is represented by

$$\mathbf{x} = \sum_{i=1}^3 h_i(r, s) \mathbf{x}_i \quad \text{with} \quad \mathbf{x}_i = [x_i \quad y_i]^T, \quad (1)$$

and

$$h_1 = 1 - r - s, \quad h_2 = r, \quad h_3 = s, \quad (2)$$

where  $\mathbf{x}_i$  is the position vector of the  $i$ th node in the global Cartesian coordinate system, and  $h_i(r, s)$  is the two-dimensional interpolation function of the standard isoparametric finite element procedure corresponding to the  $i$ th node.

The displacement of the element is interpolated by

$$\mathbf{u} = \sum_{i=1}^3 h_i(r, s) \mathbf{u}_i \quad \text{with} \quad \mathbf{u}_i = [u_i \quad v_i]^T, \quad (3)$$

in which  $\mathbf{u}_i$  is the displacement vector of the  $i$ th node in the global Cartesian coordinate system.

The strain field within a 3-node triangular element is obtained using the standard isoparametric finite element procedure as follows:

$$\boldsymbol{\varepsilon}^{(e)} = [\varepsilon_{xx} \quad \varepsilon_{yy} \quad 2\varepsilon_{xy}]^T = \mathbf{B}^{(e)} \mathbf{u}^{(e)} \quad \text{with} \quad \mathbf{B}^{(e)} = [\mathbf{B}_1 \quad \mathbf{B}_2 \quad \mathbf{B}_3], \quad \mathbf{u}^{(e)} = [\mathbf{u}_1 \quad \mathbf{u}_2 \quad \mathbf{u}_3]^T, \quad (4)$$

where  $\mathbf{B}^{(e)}$  is the strain-displacement matrix of an element,  $\mathbf{u}^{(e)}$  is the nodal displacement vector of the element, and  $\mathbf{B}_i$  is the strain-displacement matrix corresponding to the  $i$ th node.

Then, we define smoothed strains between a target element and its neighboring elements ([Lee 2018](#))

$$\hat{\boldsymbol{\varepsilon}}^{(k)} = \frac{1}{A^{(e)} + A^{(k)}} (A^{(e)} \boldsymbol{\varepsilon}^{(e)} + A^{(k)} \boldsymbol{\varepsilon}^{(k)}) \quad \text{with} \quad k = 1, 2, 3, \quad (5)$$

in which  $\boldsymbol{\varepsilon}^{(e)}$  and  $\boldsymbol{\varepsilon}^{(k)}$  are the strains of the target element and the  $k$ th neighboring element, respectively, as shown in Fig. 1(a), and  $A^{(e)}$  and  $A^{(k)}$  are the areas of the target element and the  $k$ th neighboring element, respectively, see Fig. 1(b). For boundary edges, we use  $\hat{\boldsymbol{\varepsilon}}^{(k)} = \boldsymbol{\varepsilon}^{(e)}$ .

From Eq. (5), we directly assign the smoothed strain values to the three Gauss points (given in Fig. 1c) of the target element using the following equations, shown in Fig. 1(d) (Lee 2018):

$$\boldsymbol{\varepsilon}^a = \frac{1}{2}(\hat{\boldsymbol{\varepsilon}}^{(1)} + \hat{\boldsymbol{\varepsilon}}^{(3)}), \quad \boldsymbol{\varepsilon}^b = \frac{1}{2}(\hat{\boldsymbol{\varepsilon}}^{(1)} + \hat{\boldsymbol{\varepsilon}}^{(2)}), \quad \boldsymbol{\varepsilon}^c = \frac{1}{2}(\hat{\boldsymbol{\varepsilon}}^{(2)} + \hat{\boldsymbol{\varepsilon}}^{(3)}). \quad (6)$$

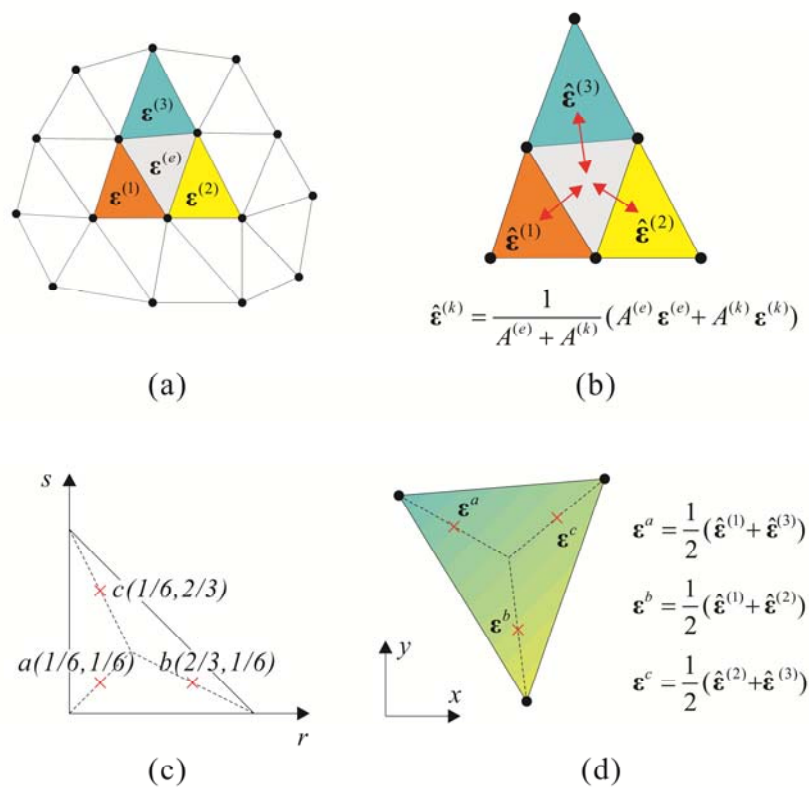


**Fig. 1.** Application of the strain-smoothed element method to the 3-node triangular element: (a) Strains of a target element and its neighboring elements. (b) Strain smoothing between the target element and each neighboring element. (c) Three Gauss points. (d) Construction of the smoothed strain field through the three Gauss points.

To investigate the performance of the smoothed 3-node triangular element adopting the SSE method, a 2D block problem is considered as shown in Fig. 2. We apply a distributed compression force of total magnitude  $P=1$  at the right half of the top edge and its bottom edge is clamped. Plane stress conditions are considered with the Young's modulus  $E=3 \times 10^7$  and Poisson's ratio  $\nu=0.3$ . The solutions are obtained with meshes of  $N \times N$  elements ( $N=2, 4, 8,$  and  $16$ ).

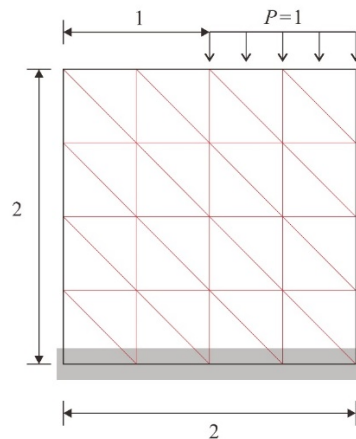


**Fig. 2.** 2D block problem (4 by 4 mesh).

**Fig. 3** shows the convergence curves obtained using the energy norm. We obtain the reference solutions using a  $32 \times 32$  mesh of 9-node 2D solid elements. The element size in the convergence curves is defined as  $h = 1/N$ . The element adopting the SSE method shows significantly improved accuracy.

The strain smoothing methods achieve significant accuracy improvement without additional degrees of freedoms (DOFs), while other methods such as enriched FEM require additional DOFs (Jun 2018, Kim 2018, 2019). Similar approaches have been used in the development of the smoothed 4-node tetrahedral element. See the reference (Lee 2018) for detailed derivations and its performance.

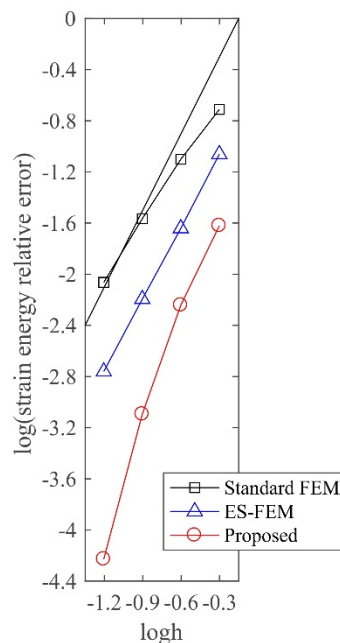


**Fig. 3.** Convergence curves for the 2D block problem. The bold line represents the optimal convergence rate.

### 3. STRAIN-SMOOTHED ELEMENT METHOD FOR SHELL ELEMENTS

The MITC3+ shell element shows almost excellent behaviors in bending-dominated problems, but its membrane performance is the same as that of the displacement-based 3-node triangular shell elements (Lee 2014, 2015, Jeon 2015, Ko 2017).

We introduce the recently developed strain-smoothed MITC3+ shell element, which improves the membrane performance of the MITC3+ shell element by adopting the SSE method (Lee 2019). The strain-smoothed MITC3+ shell element shows significantly improved membrane performance and retains the excellent bending behaviors of the MITC3+ shell element.

In order to improve its membrane behavior, the covariant membrane strain component is smoothed using the SSE method. The decomposition of the strain components is well described in (Ko 2017).

First, we obtain the covariant membrane strains of the target element,  ${}^m e_{ln}^{(e)}$ , and of the  $k$ th neighboring element,  ${}^m e_{ln}^{(k)}$ , at center of elements. Then, the strain of the neighboring element is transformed into the convected coordinates defined at the center of the target element as follows:

$${}^m \bar{e}_{ij}^{(k)} = {}^m e_{ln}^{(k)} ({}^{(e)} \mathbf{g}_i \cdot {}^{(k)} \mathbf{g}^l) ({}^{(e)} \mathbf{g}_j \cdot {}^{(k)} \mathbf{g}^n) \quad \text{with } i, j, l, n = 1, 2, \quad (7)$$

where  ${}^{(e)} \mathbf{g}_i$  and  ${}^{(k)} \mathbf{g}^l$  are the covariant base vectors of the target element and the contravariant base vectors of the  $k$ th neighboring element, respectively.

The smoothed membrane strain between the target and the  $k$ th neighboring elements is obtained by (Lee 2019)

$${}^m \hat{e}_{ij}^{(k)} = \frac{1}{A^{(e)} + \bar{A}^{(k)}} ({}^m e_{ij}^{(e)} A^{(e)} + {}^m \bar{e}_{ij}^{(k)} \bar{A}^{(k)}) \quad \text{with } i, j = 1, 2, \quad (8)$$

and

$$\bar{A}^{(k)} = (\mathbf{n}^{(e)} \cdot \mathbf{n}^{(k)}) A^{(k)}, \quad \mathbf{n}^{(e)} = {}^{(e)} \mathbf{g}_3 / \|{}^{(e)} \mathbf{g}_3\|, \quad \mathbf{n}^{(k)} = {}^{(k)} \mathbf{g}_3 / \|{}^{(k)} \mathbf{g}_3\|, \quad (9)$$

where  $A^{(e)}$  and  $A^{(k)}$  are the mid-surface areas of the target and the  $k$ th neighboring elements, respectively,  $\mathbf{n}^{(e)}$  and  $\mathbf{n}^{(k)}$  are the unit normal vectors defined at the centers of the target and neighboring elements, respectively, and  $\bar{A}^{(k)}$  is the projected area. For the boundary edges,  ${}^m \hat{e}_{ij}^{(k)} = {}^m e_{ij}^{(e)}$ .

Then, we assign the membrane strains in Eq. (8) to the three Gauss points using the following equations (Lee 2019)

$${}^m e_{ij}^{(A)} = \frac{1}{2} ({}^m \hat{\epsilon}_{ij}^{(3)} + {}^m \hat{\epsilon}_{ij}^{(1)}), \quad {}^m e_{ij}^{(B)} = \frac{1}{2} ({}^m \hat{\epsilon}_{ij}^{(1)} + {}^m \hat{\epsilon}_{ij}^{(2)}), \quad {}^m e_{ij}^{(C)} = \frac{1}{2} ({}^m \hat{\epsilon}_{ij}^{(2)} + {}^m \hat{\epsilon}_{ij}^{(3)}),$$

with  $i, j = 1, 2$ . (10)

The smoothed covariant membrane strain in Eq. (10) replaces the covariant membrane strain. We use the originally defined covariant bending strains, and for the covariant transverse shear strains, the assumed strains of the MITC3+ shell element are used (Lee 2014, 2015).

In order to verify the performance of the smoothed MITC3+ shell element, we consider the Scordelis-Lo roof shell problem (Lee 2002, Chapelle 2010) shown in Fig. 4. The structure is a part of a cylinder which has length  $L=25$ , radius  $R=25$ , and uniform thickness  $t$ . A self-weight loading  $f_z=80$  per unit area is acting on the structure.  $E=4.32 \times 10^8$  and  $\nu=0$  are assumed.

Both ends of the shell structure are supported by rigid diaphragms. Considering the symmetry, only one-quarter is considered with the following boundary conditions:  $u_x = u_z = 0$  along AC,  $u_y = \alpha = 0$  along BD and  $u_x = \beta = 0$  along CD. We consider the  $N \times N$  element meshes with  $N = 8, 16$ , and 32.

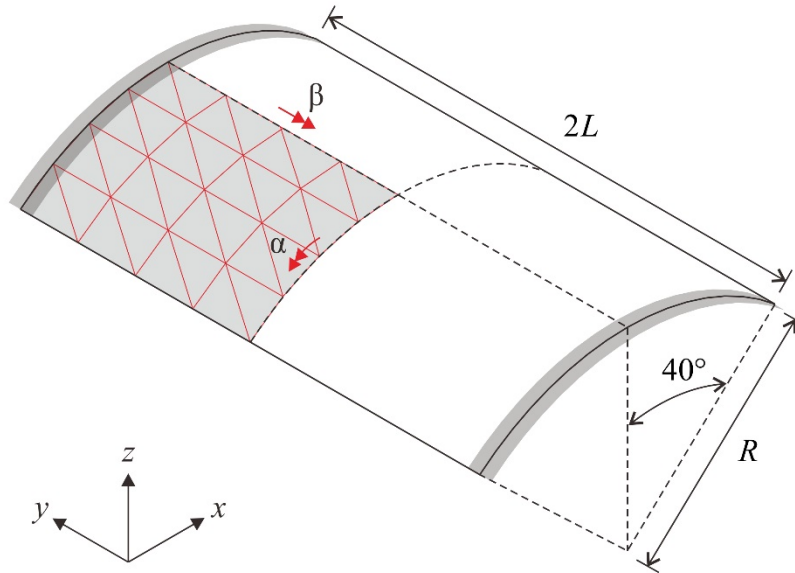
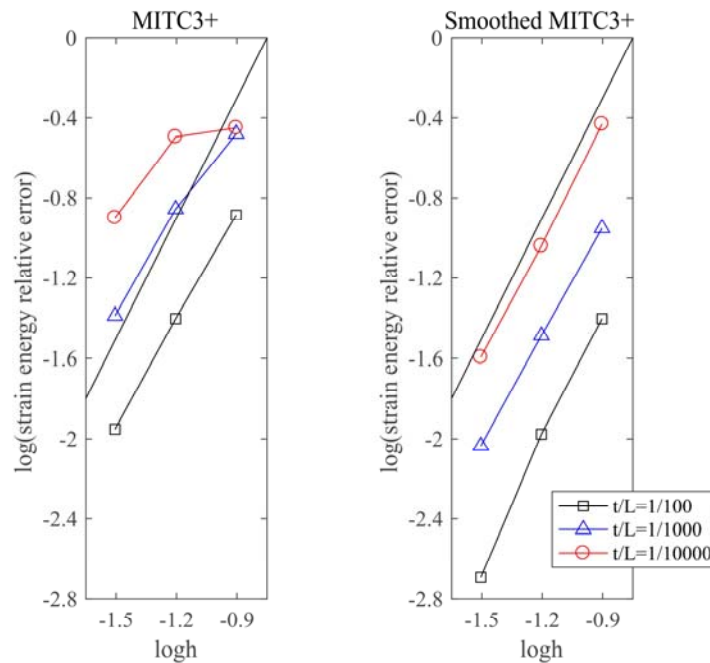


Fig. 4. Scordelis-Lo roof shell problem (4 by 4 mesh).



**Fig. 5.** Convergence curves for the Scordelis-Lo roof shell problem. The bold line represents the optimal convergence rate.

**Fig. 5** shows the convergence curves of the MITC3+ shell element, the enriched MITC3+ shell element and the smoothed MITC3+ shell element obtained using the energy norm. Three different thickness to length ratios:  $t/L = 1/100$ ,  $1/1000$  and  $1/10000$ ) are considered. The reference solutions are obtained using a  $64 \times 64$  mesh of MITC9 shell finite elements. The element size is  $h = 1/N$ . The smoothed MITC3+ shell finite element gives significantly improved solutions comparable to the enriched MITC3+ shell element.

#### 4. CONCLUSIONS

In this paper, we introduced the strain-smoothed 3-node triangular and 4-node tetrahedral solid elements and the strain-smoothed MITC3+ shell element adopting the SSE method. The smoothed elements passed the isotropy, patch and zero energy mode tests. Through numerical examples, we verified that the proposed elements show significantly improved convergence behaviors. Also, the SSE method could be easily extended for solving non-linear problems.

#### REFERENCES

- Liu, G.R., Nguyen-Thoi, T., Lam, K.Y. (2009), "An edge-based smoothed finite element method (ES-FEM) for static, free and forced vibration analyses of solids," *J. Sound Vib.*, **320**, 1100-30.

- Liu, G.R., Nguyen-Thoi, T., Nguyen-Xuan, H., Lam, K.Y. (2009), "A node-based smoothed finite element method (NS-FEM) for upper bound solutions to solid mechanics problems," *Comput. Struct.*, **87**, 14–26.
- Sohn, D., Han, J., Cho, Y.S., Im, S. (2013), "A finite element scheme with the aid of a new carving technique combined with smoothed integration," *Comput. Methods Appl. Mech. Eng.*, **254**, 42–60.
- Shin, C.M., Lee, B.C. (2014), "Development of a strain-smoothed three-node triangular flat shell element with drilling degrees of freedom," *Finite Elem. Anal. Des.*, **86**, 71–80.
- Lee, C., Kim, H., Im, S. (2016), "Polyhedral elements by means of node/edge-based smoothed finite element method," *Int. J. Numer. Methods Eng.*, **110**, 1069–1100.
- Lee, C., Kim, H., Kim, J., Im, S. (2017), "Polyhedral elements using an edge-based smoothed finite element method for nonlinear elastic deformations of compressible and nearly incompressible materials," *Comput. Mech.*, **60**, 659–682.
- Lee, C., Lee, P.S. (2018), "A new strain smoothing method for triangular and tetrahedral finite elements," *Comput. Methods Appl. Mech. Eng.*, **341**, 939-955.
- Lee, C., Lee, P.S. (2019), "The strain-smoothed MITC3+ shell finite element," *Comput. Struct.*, **223**.
- Jun, H., Yoon, K., Lee, P.S., Bathe, K.J. (2018), "The MITC3+ shell element enriched in membrane displacements by interpolation covers," *Comput. Methods Appl. Mech. Eng.*, **337**, 458-80.
- Kim, S., Lee, P.S. (2018), "A new enriched 4-node 2D solid finite element free from the linear dependence problem," *Comput. Struct.*, **202**, 25-43.
- Kim, S., Lee, P.S. (2019), "New enriched 3D solid finite elements: 8-node hexahedral, 6-node prismatic, and 5-node pyramidal elements," *Comput. Struct.*, **216**, 40-63.
- Lee, Y., Lee, P.S., Bathe, K.J. (2014), "The MITC3+ shell element and its performance," *Comput. Struct.*, **138**, 12-23.
- Lee, Y., Jeon, H.M., Lee, P.S., Bathe, K.J. (2015), "The modal behavior of the MITC3+ triangular shell element," *Comput. Struct.*, **153**, 148-64.
- Jeon, H.M., Lee, Y., Lee, P.S., Bathe, K.J. (2015), "The MITC3+ shell element in geometric nonlinear analysis," *Comput. Struct.*, **146**, 91-104.
- Ko, Y., Lee, Y., Lee, P.S., Bathe, K.J. (2017), "Performance of the MITC3+ and MITC4+ shell elements in widely-used benchmark problems," *Comput. Struct.*, **193**, 187-206.
- Ko, Y., Lee, P.S., Bathe, K.J. (2017), "A new 4-node MITC element for analysis of two-dimensional solids and its formulation in a shell element," *Comput. Struct.*, **192**, 34-49.
- Lee, P.S., Bathe, K.J. (2002), "On the asymptotic behavior of shell structures and the evaluation in finite element solutions," *Comput. Struct.*, **80**, 235–55.
- Chapelle, D., Bathe, K.J. (2010), "The finite element analysis of shells-Fundamentals," *Springer Science & Business Media*.